

Effective conductivity in a lattice model for heterogeneous materials with complex distributions of grain sizes

R. PIASECKI¹⁾

Institute of Chemistry, University of Opole, Oleska 48, PL 45-052 Opole, Poland

Abstract

A modified version of coarsened square lattice model proposed recently [phys. stat. sol. (b) **209**, 403 (1998)] for two-phase granular conductors is examined in the context of effects of various types of grain size distributions on the concentration dependent overall conductivity. The modification relates to limiting the bond conductivities to the two pure ones and the mixed one, which value is highly sensitive to local concentrations of both phases. Differently shaped grains are also allowed. By controlling the polydispersity in grain sizes and their relative area frequencies the effective conductivity in such composite systems can be enhanced or reduced.

PACS numbers: 05.90.+m, 72.80.Tm

Recently, a lattice model with pure and mixed random bonds for effective conductivity of binary granular systems has been proposed [1]. A network extension [2] of effective-medium approximation (EMA) was adapted as the simplest technique embodying the essential physics of macroscopic properties of random heterogeneous materials (RHMs) [3]. The non-trivial critical behaviour of the conductor-insulator and conductor-superconductor systems was demonstrated for certain grain size distributions (GSDs). Within this approach every grain for H-(L-phase) of high σ^H (low σ^L) conductivity is composed of grains of type '1' $\equiv s_1$ which can 'occupy' the centre alone of a unit bond on *coarsened* square lattice marking a pure H-(L-bond). The effective electrical conductivity $\sigma^*(p)$, where p is the fraction of unit H-bonds, was considered only for systems with simple in form grains. We propose a modification of that model which allows also *differently* shaped grains and *complex* GSDs. This may gain an insight how to use such experimental information to describe effective properties of RHMs.

Consider the coarsened square lattice with bonds each of length $l > 1$. To each of the bonds a square model-cell is assigned consisting of l^2 'positions', i.e., the centres of *neighbouring* unit bonds, see Fig.1 in [1]. Now, besides square shape, e.g., for '4' $\equiv s_4$ grains, one allows also rodlike or T-like grains, letter L or 'zigzag' shaped grains and their mirror reflections. We notice that insulating mono-sized square and rodlike particles were considered for particle-size effect on the conductivity of dispersed ionic conductors [4]. Given that area of s_n grain is 'measured' by the number n of the occupied positions, the 'shake' rule used in numerical simulations reads: the sum of all H and L-grain areas inside of every model-cell must be equal to l^2 . Let N and $N^K(p)$, for a given p , be the number of all bonds and bonds of type $K = H, L$ and M (we comment further on mixed case below). The bond fractions defined as $F_K(p) \equiv N^K(p)/N$ fulfil the obvious condition

$$F_H(p) + F_M(p) + F_L(p) = 1. \quad (1)$$

¹⁾ e-mail: piaser@uni.opole.pl

Similarly to [1], $\gamma_i \equiv n_i/l^2$ and $1 - \gamma_i$ is the local fraction of n_i and $l^2 - n_i$ of unit H and L-bonds in i -th model-cell. Thus for a pure H-(L-bond) we have $\gamma_i = 1$ ($= 0$) while for i -th M-bond $0 < \gamma_i < 1$. Now, for the fraction of unit H-bonds the elementary relation holds

$$p = \frac{1}{N} [N^H(p) + \sum_{i \in \{M\}} \gamma_i] \equiv F_H(p) + \gamma(p) F_M(p) , \quad (2)$$

where $\gamma(p)$ is an *average* fraction of unit H-bonds per mixed-cell. In order to simplify the problem the following approximation is made: each of i -th mixed-cells with a certain σ_i^M conductivity can be replaced by a representative mixed-cell with $\gamma(p)$ and $1 - \gamma(p)$ fractions of H and L-bonds, and the mixed $\sigma^M(p)$ conductivity be calculated within the EMA from a corresponding quadratic expression $(\sigma^M)^2 + \sigma^M(\sigma^H - \sigma^L)(1 - 2\gamma(p)) - \sigma^H\sigma^L = 0$. Thus

$$\sigma^M(p) = \left[-(\sigma^H - \sigma^L)(1 - 2\gamma(p)) + \sqrt{(\sigma^H - \sigma^L)^2(1 - 2\gamma(p))^2 + 4\sigma^H\sigma^L} \right] / 2 . \quad (3)$$

The distribution of the corresponding bond conductivities $\sigma^L < \sigma^M(p) < \sigma^H$ is given by

$$P(\sigma) = F_H(p) \delta(\sigma - \sigma^H) + F_M(p) \delta(\sigma - \sigma^M(p)) + F_L(p) \delta(\sigma - \sigma^L) . \quad (4)$$

Following [2] the equation for the overall effective conductivity $\sigma^*(p)$ can be now written as

$$F_H(p) \frac{\sigma^H - \sigma^*(p)}{\sigma^H + \sigma^*(p)} + F_M(p) \frac{\sigma^M(p) - \sigma^*(p)}{\sigma^M(p) + \sigma^*(p)} + F_L(p) \frac{\sigma^L - \sigma^*(p)}{\sigma^L + \sigma^*(p)} = 0 . \quad (5)$$

Note, that the fractions $F_H(p)$, $F_M(p)$ and $F_L(p)$ are difficult to calculate analytically due to large number of possible local configurations in a model-cell. The same refers to $\gamma(p)$ function. However, using Eqs.(1) and (2) at least two of the four quantities can be treated as *independent* ones, for instance, $F_M(p)$ and $\gamma(p)$. Thus, from Eqs.(1) and (2) we have

$$F_H(p) = p - \gamma(p) F_M(p) \quad \text{and} \quad F_L(p) = (1 - p) - (1 - \gamma(p)) F_M(p) . \quad (6a, b)$$

As observed in numerical simulations for various GSDs the fractions $F_H(p)$ and $F_L(p)$ are concave functions while the mixed fraction $F_M(p)$ is a convex one reaching a maximum, say β , at certain $p = \alpha$. The topological equivalence of equally sized H and L-grains implies $\alpha = 0.5$ while for complex GSDs we expect $\alpha \neq 0.5$. Let a trial function approximates $F_M(p)$

$$F_M(p) \approx \begin{cases} a_0 + a_1 p + a_2 p^2 & \text{for } 0 < p < \alpha , \\ \beta & \text{for } p = \alpha , \\ b_0 + b_1 p + b_2 p^2 & \text{for } \alpha < p < 1 , \end{cases} \quad (7)$$

where constant coefficients a_k and b_k can be determined from the conditions imposed below

- (i) $\lim_{p \rightarrow 0^+} F_M(p) = 0$ and $\lim_{p \rightarrow 1^-} F_M(p) = 0$,
- (ii) $\lim_{p \rightarrow \alpha^-} F_M(p) = \lim_{p \rightarrow \alpha^+} F_M(p) = \beta$,
- (iii) $\lim_{p \rightarrow \alpha^-} \frac{dF_M(p)}{dp} = \lim_{p \rightarrow \alpha^+} \frac{dF_M(p)}{dp} = 0$.

The final form is

$$F_M(p) = \begin{cases} \left[1 - \left(\frac{\alpha - p}{\alpha}\right)^2\right] \beta \equiv [2\alpha p - p^2] \beta / \alpha^2 & \text{for } 0 < p \leq \alpha, \\ \left[1 - \left(\frac{p - \alpha}{1 - \alpha}\right)^2\right] \beta \equiv [1 - 2\alpha + 2\alpha p - p^2] \beta / (1 - \alpha)^2 & \text{for } \alpha \leq p < 1. \end{cases} \quad (9)$$

From Eqs.(6a,b) and (9) the remaining $F_H(p)$ and $F_L(p)$ bond fractions can be also parameterized by α , β and $\gamma(p)$. At this stage, we concentrate on numerical evaluation of model functions for certain GSDs. The numerical simulations on a square lattice with 4900 bonds each of length $l = 6$ were performed for $p = 0.1, 0.2, \dots, 0.9$. The probability a grain of given type is randomly selected was proportional to the area fraction of that type.

First, we distinguish the two cases: (I) $s_4, s_9, s_{16}, s_{25}, s_{36}$ distribution with the relative area frequencies $f_i(H) \approx 0.046, 0.153, 0.454, 0.227, 0.120$ depicted in the inset, filled squares, in Fig. 1(a), and s_1 one for L-grains; (I-r) the reverse case with the interchanged GSDs. For both cases the averaged over 1000-run trials $\sigma^*(p)$ values are shown in Fig. 1(a), top and bottom dashed lines. We see, that polydispersed in size H-grains when embedded into a matrix of mono-sized L-grains favour a higher effective conductivity than for case (I-r). With a high accuracy same results are obtained by first averaging $F_K(p)$ fractions and then solving Eq.(5).

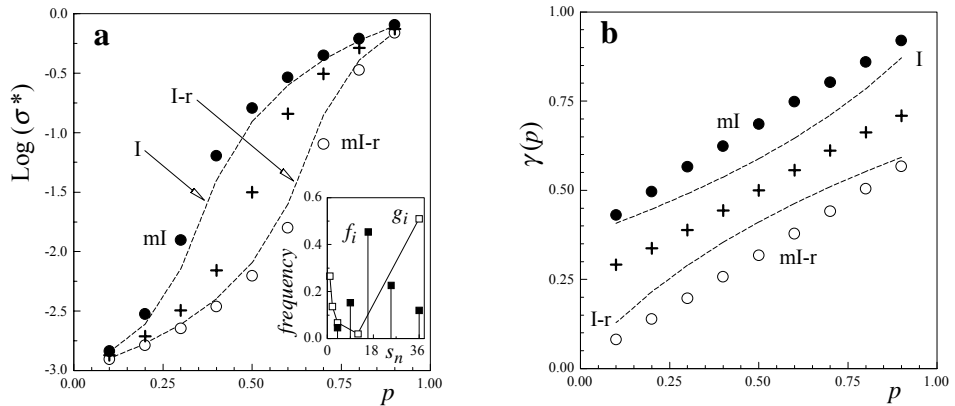


Fig. 1. Examples of GSD dependence for numerically calculated model quantities at length scale $l = 6$. Left: the effective conductivity $\text{Log}(\sigma^*(p))$ for $\sigma^H = 1$ and $\sigma^L = 10^{-3}$ in a.u. For case (I) with $[f_i(H); s_1(L)]$, top dashed line, for case (I-r) with $[s_1(H); f_i(L)]$, bottom dashed line, for case (mI) with $[f_i(H); g_i(L)]$, filled circles, for case (mI-r) with $[g_i(H); f_i(L)]$, open circles, and at scale $l = 4$, for case (II) with $[s_1(H); s_1(L)]$, “+”. For f_i , and g_i frequencies, see the inset (a); right: the corresponding $\gamma(p)$ values (b)

Next, we replace $s_1(L)$ by $s_1, s_2, s_4, s_{12}, s_{36}$ distribution with the relative area frequencies $g_i(L) \approx 0.265, 0.136, 0.068, 0.021, 0.510$ depicted in the inset, open squares, in Fig. 1(a). This way we obtain case (mI), i.e., the modified case (I). Now, the clear increase of $\sigma^*(p)$ with regard to case (I) appears in Fig. 1(a), filled circles. Quite surprisingly, the presence of the largest s_{36} L-grains seem to be necessary for that. In turn, having interchanged GSDs in case (mI) we mark it as (mI-r). For this case the largest reduction of $\sigma^*(p)$ can be seen in Fig. 1(a),

open circles. Such a dependence of $\sigma^*(p)$ on GSDs can be understood on the basis of Figs. 1(b) and 2(a), where the corresponding $\gamma(p)$ functions (with the inversion symmetry of the appropriate pairs with respect to point $(p=0.5, \gamma=0.5)$) and mixed-bond fractions (with the reflection symmetry under the replacement $p \leftrightarrow 1-p$) are presented. Let the arrows \uparrow and \downarrow symbolise an increasing and decreasing values of quantities followed by them and, for a given p , consider exemplary ‘transition’: (I) \rightarrow (ml). This implies $F_H \uparrow, F_M \downarrow, F_L \uparrow, \gamma \uparrow, \sigma^M \uparrow$ and finally $\sigma^* \uparrow$. Such a behaviour is a peculiar feature of our model in which a spatial distribution of mixed-cells with various conductivities σ_i^M is approximated by same distribution but of identical ‘average’ mixed-cells each of the effective $\sigma^M(p)$, for given p and GSDs. For other GSDs (given that p is still fixed) $\sigma^M(p)$ varies through $\gamma(p)$ function. A similarity between $\gamma(p)$ behaviour, e.g., at scale $l=4$ for additional case (II) with $s_1(H)$ and $s_1(L)$, see symbols ‘+’ in Fig. 1(b), and the so called microstructure parameters ζ_1 (see Tab. I) and η_1 (Tab. IX) in [5], might be not incidental. Finally, in Fig. 2(b) we show the entropic measure $S_\Delta(p) = -l^2 \{p \ln p + (1-p) \ln(1-p) - F_M(p)[\gamma(p) \ln \gamma(p) + (1-\gamma(p)) \ln(1-\gamma(p))]\}$ of spatial inhomogeneity [6] given here in the thermodynamic limit. Let us compare in this figure i) case (I) with (ml), and ii) (I-r) with (ml-r). Remembering that both modifications were done by replacing s_1 with $s_1, s_2, s_4, s_{12}, s_{36}$, due to the reduced F_M for both i) and ii) and proper behaviour of $\gamma(p)$ and $1-\gamma(p)$ functions we observe the higher spatial inhomogeneity for the two modifications. Also, in Fig. 2(b) at scale $l=6$, the asymmetry of the S_Δ curves regarding $p=0.5$ confirms the topological inequivalence of H and L-phases [7] in contrast to the symmetrical case (II) at scale $l=4$ with equally mono-sized grains, $s_1(H)$ and $s_1(L)$.

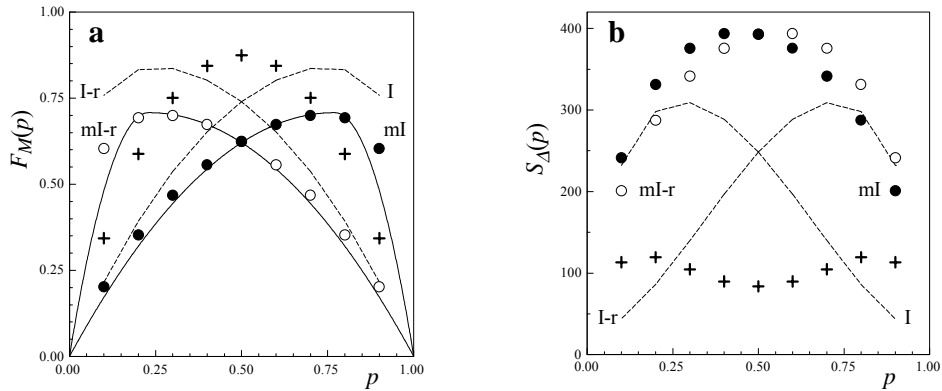


Fig. 2. Further examples of GSD dependence for the model related quantities with referring to Fig. 1 notation. Left: the fractions of mixed bonds $F_M(p)$ with an analytical result Eq.(9) for both modified cases with estimated $\alpha \approx 0.77$ for (ml) and $\alpha \approx 0.27$ for (ml-r) and common $\beta \approx 0.71$, solid lines (a); right: the corresponding coarsened lattice spatial inhomogeneity quantified by entropic measure $S_\Delta(p)$ in the thermodynamic limit [6]. The S_Δ values for case (II) were 60 times enlarged, symbols ‘+’ (b)

Apart from the simplicity of the model, a wide variety of grain areas is included. A porosity of composite media can be readily incorporated to this model. Thus, it exhibits information not necessarily revealed (within EMA) by other models of RHMs.

References

- [1] R. PIASECKI, phys. stat. sol. (b) **209**, 403 (1998), and references therein, cond-mat/0005386.
- [2] S. KIRKPATRICK, Rev. Mod. Phys. **45**, 574 (1973).
- [3] S. TORQUATO, Random Heterogeneous Materials. Microstructure and Macroscopic Properties, Springer-Verlag New York 2002.
- [4] H.E. Roman, M. Yussouff, Phys. Rev. B **36**, 7285 (1987).
- [5] A.P. Roberts, M. Teubner, Phys. Rev. E **51**, 4141 (1995).
- [6] R. PIASECKI, Physica A **277**, 157 (2000), cond-mat/0008313; Surf. Sci. **454–456**, 1058 (2000), cond-mat/0008470.
- [7] R. PIASECKI, A. Czaiński, phys. stat. sol. (b) **217**, R10 (2000), cond-mat/0008334.